

## Review

## Condensed complexes of cholesterol and phospholipids

Harden M. McConnell\*, Arun Radhakrishnan

*Department of Chemistry, Stanford University, Stanford, CA 94305, USA*

Received 10 April 2002; received in revised form 5 September 2002; accepted 5 September 2002

**Abstract**

There is overwhelming evidence that lipid bilayer regions of animal cell membranes are in a liquid state. Quantitative models of these bilayer regions must then be models of liquids. These liquids are highly non-ideal. For example, it has been known for more than 75 years that mixtures of cholesterol and certain phospholipids undergo an area contraction or condensation in lipid monolayers at the air–water interface. In the past 3 years, a thermodynamic model of “condensed complexes” has been proposed to account for this non-ideal behavior. Here we give an overview of the model, its relation to other models, and to modern views of the properties of animal cell membranes. © 2003 Elsevier Science B.V. All rights reserved.

**Keywords:** Monolayer; Phase diagram; Cholesterol regulation; Short-range order; Membrane; Fatty acid

**1. Introduction***1.1. Liquid–liquid immiscibility*

There has been long-standing interest in the physical chemical properties of defined mixtures of cholesterol and phospholipids in monolayer and bilayer membranes. These quasi two-dimensional mixtures are of intrinsic interest to physical chemists. They also provide insight into certain properties of the membranes of animal cells. One of the early studies is that of Leathes [1] who studied these mixtures in monolayers at the air–water interface. This investigator found that binary mixtures of cholesterol and egg-lecithin have average molecular areas that are much smaller than expected for ideal mixtures. This was referred to as the cholesterol “condensing” effect. Later it was proposed that cholesterol and phospholipids form complexes with specific stoichiometries [2–6]. On the other hand, subsequent investigators have suggested that specific complexes are not needed to understand the properties of these mixtures [7–9]. There have also been a number of proposals for lattice-based structures of mixtures having specific compositions [10–12]. The book edited by Feingold [13] summarizes the status of models for these mixtures up until 1993.

In 1987, it was reported that two immiscible liquid phases can be formed from binary mixtures of cholesterol and dimyristoylphosphatidylcholine (DMPC) in monolayers [14]. This finding had been anticipated from earlier observations and speculations concerning these mixtures in bilayers [13,15–17]. The observation of immiscible liquid phases made possible quantitative studies of their properties, including phase diagrams, long-range intermolecular electrostatic dipole forces, and monolayer hydrodynamics [18]. Fig. 1 shows an epifluorescence view of a binary mixture of cholesterol and DMPC. The dark liquid is rich in cholesterol, and the more fluorescent liquid is rich in phospholipid. The monolayer contains a low concentration (0.2 mol%) of fluorescent phospholipid probe. This probe dissolves preferentially in the phospholipid-rich phase. In this monolayer, the composition is such that there are approximately equal areas of the two phases, and there is frequent contrast inversion, namely dark domains on a light background, and light domains on a dark background. In Fig. 1A, the pressure is low and the domains are circular in shape. When the pressure is increased, the two phases merge into one, and the pressure, and composition (and temperature) at this transition from two phases to one defines a point on the phase boundary. When the monolayer has a composition close to the critical composition, the domains generally form stripes as the monolayer pressure approaches the critical pressure [19]. Stripes are illustrated in Fig. 1B. In many of the experiments, dihydrocholesterol (Dchol) is used instead of cholesterol to avoid air and photooxidation. It has been

\* Corresponding author. Tel.: +1-650-723-4571; fax: +1-650-723-4943.  
E-mail address: [harden@stanford.edu](mailto:harden@stanford.edu) (H.M. McConnell).

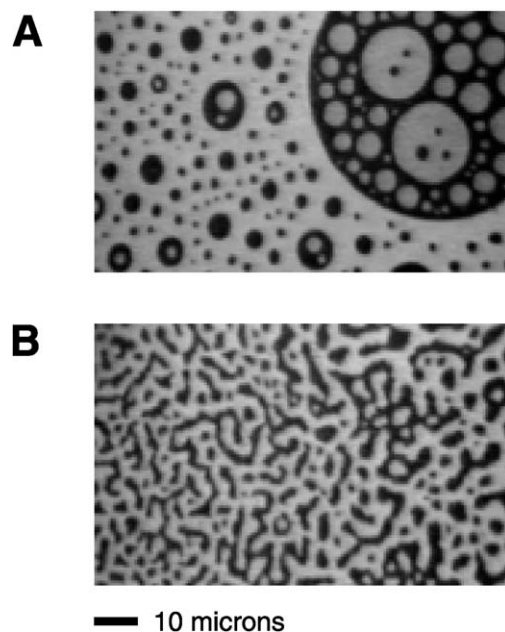


Fig. 1. Epifluorescence micrographs of a lipid monolayer consisting of a binary mixture of DMPC and Dchol at an air–water interface at room temperature (23 °C). The monolayers contain 69.8 mol% DMPC, 30 mol% Dchol and 0.2 mol% of a fluorescently labeled phospholipid (Texas Red–dihexanoylphosphatidylethanolamine—TR-DHPE). This probe provides contrast between phases. (A) Image of monolayer at a surface pressure of 2 dyn/cm showing two-phase coexistence, where the dark phase is a Dchol-rich liquid and the brighter phase is a DMPC-rich liquid. The domains are 5–10  $\mu$  in diameter and exhibit Brownian motion. (B) Image of monolayer at a surface pressure of 9.4 dyn/cm showing the stripe phase characteristic of proximity to a miscibility critical point. The stripes become thinner and disappear at a surface pressure of 9.5 dyn/cm and only one homogeneous phase is observed at higher pressures.

found that using Dchol instead of cholesterol yields slightly lower values of the phase transition pressures, but the phase behavior of the two sterols is virtually identical otherwise [20,21]. Controls are always carried out using cholesterol in a chamber flooded with argon gas and with an argon-saturated aqueous subphase.

The early phase diagrams reported for cholesterol–phospholipid mixtures in monolayers are qualitatively similar to diagrams well known for three-dimensional liquid mixtures [22]. Fig. 2A gives an experimental phase diagram for a binary mixture of Dchol and a phospholipid with two unsaturated fatty acid chains, dipalmitoleoylphosphatidylcholine (DPOPC). Domain shapes and critical fluctuations are similar to those shown in Fig. 1A and B. The experimental phase diagram can be mimicked semi-quantitatively with classical regular solution theory, as illustrated in Fig. 2B [23]. The regular solution “repulsion” between cholesterol and this phospholipid is non-specific. A thermodynamic repulsion parameter of this sort has been used to describe many common mixtures of liquids in three dimensions [22].

In monolayers, the sizes and shapes of the coexisting liquid domains are affected by intermolecular electrostatic

dipole–dipole forces. These forces play a role in the formation of the stripe phase illustrated in Fig. 1B [19]. Long-range components of the forces are weak compared to chemically important forces at short-range. Nonetheless, the long-range dipole fields in monolayers serve as revealing probes of the molecular and thermodynamic properties of these mixtures. The dipoles also provide a means for manipulating molecules with externally applied fields [24]. The relatively weak long-range electrostatic forces are not important in lipid bilayers or cell membranes, and are probably not observable due to screening.

Two-dimensional monolayer flow is easily observed using epifluorescence microscopy when there are coexisting liquid domains. Observations demonstrate unambiguously that these phases are liquids, at least for monolayers where the coexisting phases persist. In monolayers at lower pressures, the hydrodynamics is dominated by the drag due to the aqueous subphase rather than membrane viscosity [25,26]. This is likely to be an important source of drag in bilayers as well [27,28]. These comments of course do not apply to the known solid-like (liquid condensed) phases in

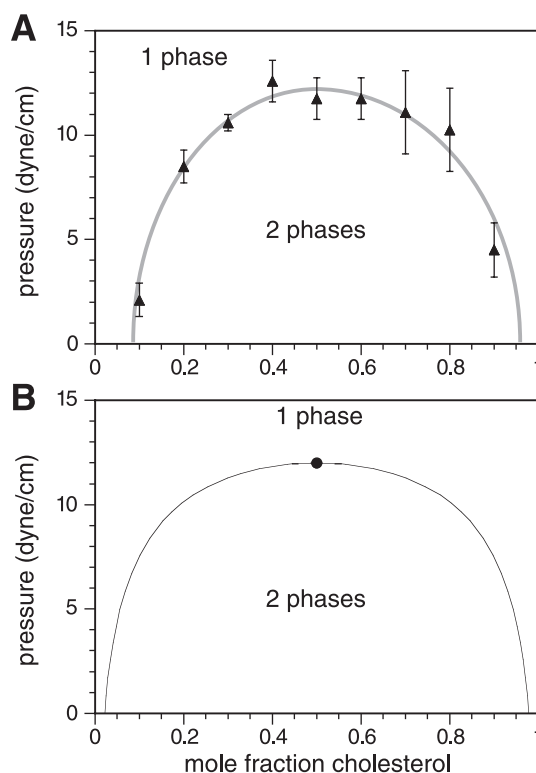


Fig. 2. Phase diagrams for a binary mixture of Dchol and a phospholipid with two unsaturated fatty acid chains, DPOPC. (A) Experimental phase diagram showing liquid–liquid immiscibility for the DPOPC/Dchol binary system (taken from Ref. [23]). There are two phases below the curve at lower pressures, and one phase above at higher pressures. Plotted data points represent the transition pressures that mark the disappearance of two-phase coexistence during monolayer compression. The gray curve is a fit to data, and is not theoretical. (B) Calculated phase diagram for a binary mixture of DPOPC and Dchol using a regular solution model involving non-specific repulsive interactions between the two components. The filled dot represents the critical point.

monolayers where there is known to be long-range orientational order [29].

## 2. The condensed complex model

### 2.1. Unusual phase diagrams—two components can form three liquids

To a good approximation, the lipids in animal cell membranes are in a liquid state. Therefore, relevant models of monolayer or bilayer mixtures of cholesterol and phospholipid must be models of liquids. At low cholesterol concentrations, some mixtures have certain (colligative) properties that are nearly ideal [30]. As discussed later, other properties, such as average molecular areas, are non-ideal even at low cholesterol concentrations. For many phospholipid–cholesterol mixtures, all properties are highly non-ideal at higher cholesterol concentrations. Models of these mixtures must account for both behaviors. The condensed complex model uses the well-known thermodynamics of *regular solutions*, together with the assumption of complex formation to account for deviations from the regular solution thermodynamics (a regular solution is one for which (a) the entropy of mixing is equal to the entropy of mixing of an ideal solution of the same composition, and (b) the energies of intermolecular interaction are expressed in terms of quadratic functions of composition). The term “condensed” is employed to indicate that the complexes are responsible for the condensing effect of cholesterol: the average area per molecule in the complex is less than would be expected from ideal mixing.

The condensed complex model arose from the discovery of an unusual phase diagram for binary mixtures of cholesterol with particular phospholipids, and with mixtures of phospholipids [31,32]. An example of this type of phase diagram is given in Fig. 3A. These mixtures are experimentally unique in that their phase diagrams show two upper miscibility critical points. Although such phase diagrams had been predicted theoretically [33,34], liquids with this property had not been observed previously (see also Ref. [35] for theoretical phase diagrams with two upper critical points but no sharp cusp). The novel finding can be described qualitatively as follows. A binary mixture of cholesterol and a specific phospholipid can form three distinct liquid phases at a fixed monolayer temperature and pressure ( $\pi$ ). One phase (P) is rich in phospholipid, one phase (C) is rich in cholesterol, and one phase (X) has an intermediate composition. As expected from the *phase rule* for binary mixtures, the three immiscible phases, P, X, and C, are not generally present simultaneously (in principle, the three phases may be simultaneously present at a specific temperature and pressure, but this has not yet been observed for a binary mixture). The phase of intermediate composition X is normally present either with the phospholipid-rich phase P, or with the cholesterol-rich phase C. That

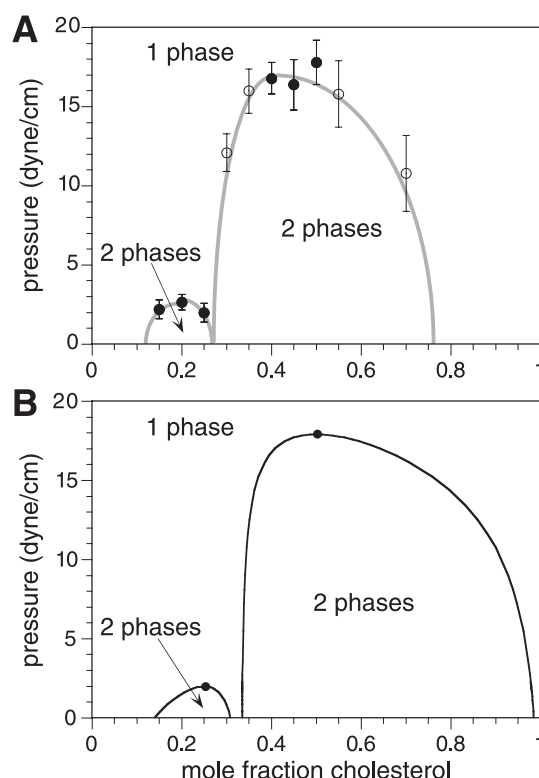


Fig. 3. Phase diagrams for a mixture of egg-sphingomyelin (SM) and cholesterol (Chol). (A) Experimental phase diagram showing liquid–liquid immiscibility for the SM/Chol system (taken from Ref. [21]). Details are the same as for Fig. 2A. Stripe superstructure phases, which represent proximity to a critical point, were observed at the transitions marked by filled circles, and not at those marked by open circles. In this case, there are two two-phase coexistence regions instead of just one as in Fig. 2, with an intervening cusp. (B) Calculated phase diagram for a mixture of cholesterol and phospholipid using a regular solution model involving repulsive interactions and where the components react to form a condensed complex. The filled dots represent critical points. The amount of complex is a maximum at the cusp composition. The two two-phase coexistence regions consist primarily of phospholipid and complex at the low cholesterol mole fractions and cholesterol and complex at the high cholesterol mole fractions. Some of the relevant parameters used are  $q=1$ ,  $p=2$ ,  $n=1$ , and  $\bar{K}=31$  (this phase diagram and a detailed discussion of the various parameters can be found in Ref. [74]).

is, the observed pairs of immiscible liquids are, P and X, or X and C. The liquid phase of intermediate composition (X) is modeled as the phase rich in condensed complex. Condensed complexes are defined in terms of the thermodynamic model of a liquid in which cholesterol and phospholipid molecules “react” reversibly with one another to form a complex of defined stoichiometry:



Here, relatively prime numbers  $p$  and  $q$  give the relative stoichiometry. The cooperativity parameter  $n$  is discussed later. The relative stoichiometry,  $q/(p+q)$ , is determined from the position of the sharp cusp in the phase diagrams. Fig. 3B shows a theoretical simulation of the data in Fig. 3A. The regular solution theory used for these simulations is

described in detail elsewhere [32]. In Fig. 3B,  $p$  and  $q$  are taken to be 2 and 1, respectively. This particular stoichiometry has been found for some but not all mixtures of cholesterol and phospholipids [36]. The simulation of the phase diagrams involves the equilibrium constant  $K$  for reaction (1). Note that this reaction is assumed to result in a contraction in area; thus the complexes are stabilized by increases of monolayer pressure. The relevance of monolayer phase diagrams such as those in Fig. 3 to bilayers, and biological membranes has sometimes been questioned, since the pressures are well below those thought to be equivalent to bilayers. However, the complexes are *stabilized* with increasing monolayer pressure. Measurements at the higher pressures have always shown complexes to be present. These measurements at the higher pressures are discussed later.

It is helpful to think of the chemical reaction (1) in terms of a titration. Starting with a liquid phospholipid membrane, consider the addition of cholesterol until its mole fraction is equal to  $q/(p+q)$ . This is the *equivalence point* where there is neither an excess of cholesterol nor an excess of phospholipid. The equivalence point is determined experimentally by the composition of the cusp in the phase diagram. As discussed later, the membrane undergoes a contraction in area as the equivalence point is approached. Also, membranes have special properties near the equivalence point(s).

Fig. 4 illustrates a significant experimental problem that commonly arises in studying phase diagrams with two two-phase regions. A representative phase diagram is shown in Fig. 4A. The two two-phase regions are designated  $\alpha$  and  $\beta$ . In the  $\alpha$  two-phase region, the domain shapes and critical point behaviors are similar to those discussed earlier in connection with Figs. 1 and 2. This is illustrated in Fig. 4B and C. On the other hand, the  $\beta$  two-phase region presents some difficulties. First, the domains tend to be quite small (1–5  $\mu\text{m}$ ), and many are probably below the resolution of the light microscope (see Fig. 4D). Due to this small size, it is difficult to see the striping associated with proximity to a critical point. This problem is circumvented experimentally by fusing a number of the small domains to form a large domain, using a non-uniform externally applied electric field. The field is then switched off and the behavior of the domain observed with increasing pressure. This procedure is illustrated in Fig. 4E. At the higher pressure, the (fused) large domain begins to exhibit the shape instability characteristic of proximity to a critical point [26] (Domain shapes depend exponentially on the ratio of the line tension to the square of the dipole density difference between the coexisting phases [18]. As the critical point is approached, the line tension approaches zero more rapidly than the square of the dipole density difference, leading to a thinning or striping of domain shapes [19]). Note also that in the  $\alpha$  two-phase region, the fluorescent probe preferentially labels the phospholipid phase, not the complex phase. In the  $\beta$  two-phase region, the probe preferentially labels the complex phase. Thus, the condensed complex phase is dark in Fig. 4B and C, but bright in Fig. 4D and E [37].

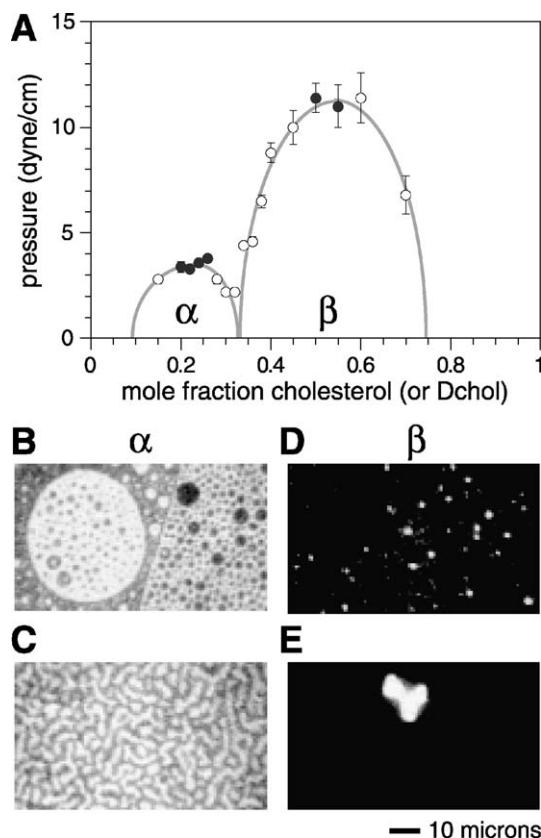


Fig. 4. Epifluorescence micrographs of monolayers of lipid mixtures with phase diagrams similar to those in Fig. 3 at an air–water interface at room temperature. The monolayers contain a binary mixture of Dchol (mole fraction  $x$ ), and phospholipids (mole fraction  $1-x$ ). The phospholipid is a 2:1 molar mixture of DMPS and DMPC. (A) Experimental phase diagram showing liquid–liquid immiscibility for the 2:1 DMPS:DMPC/Dchol system (taken from Ref. [32]). Details are the same as for Fig. 3A. The two-phase coexistence region at low Dchol mole fractions is labeled  $\alpha$ , and the one at high Dchol mole fractions is labeled  $\beta$ . (B) Image of monolayer consisting of 25 mol% Dchol, 74.8 mol% of a 2:1 ratio of DMPS:DMPC, and 0.2 mol% of the fluorescent probe, TR-DHPE at a surface pressure of 2 dyn/cm. The domains are  $\sim 5 \mu\text{m}$  in diameter and exhibit Brownian motion. (C) Image at a surface pressure of 3.2 dyn/cm for the same lipid monolayer as in B showing the stripe phase indicative of proximity to a critical point. The stripes disappear completely at 3.3 dyn/cm, and a single homogeneous phase is present at all higher pressures up to 40 dyn/cm. (D) Image of monolayer containing 50 mol% Dchol, 49.8 mol% of a 2:1 ratio of DMPS:DMPC, and 0.2 mol% of TR-DHPE at a surface pressure of 6 dyn/cm. The domains in this two-phase immiscibility region are 1–5  $\mu\text{m}$  in diameter. (E) Image at a pressure of 11.8 dyn/cm for the same lipid monolayer as in D showing the stripe phase indicative of proximity to a critical point. An inhomogeneous electric field was used to fuse domains in order to better observe if critical fluctuations occurred or not.

## 2.2. Condensation due to complex formation

The condensation effect discovered by Leathes [1] provides one of the simplest, most sensitive and direct methods for detecting condensed complexes, given the assumption that condensation is due to complex formation. Other physical measurements (phase diagrams, chemical activity and the electric field effect) point more directly to com-



plexes, but they are more challenging experimentally. In this section, emphasis is placed on area condensation. Measurements of average area as a function of cholesterol composition are carried out at a fixed pressure [21]. The data can also be taken directly from pressure–area measurements for

a series of compositions, a type of experiment carried out by many investigators [30,38,39].

Fig. 5 gives illustrative experimental data for average molecular areas. Certain qualitative generalizations have emerged from such studies. In 12 different mixtures where

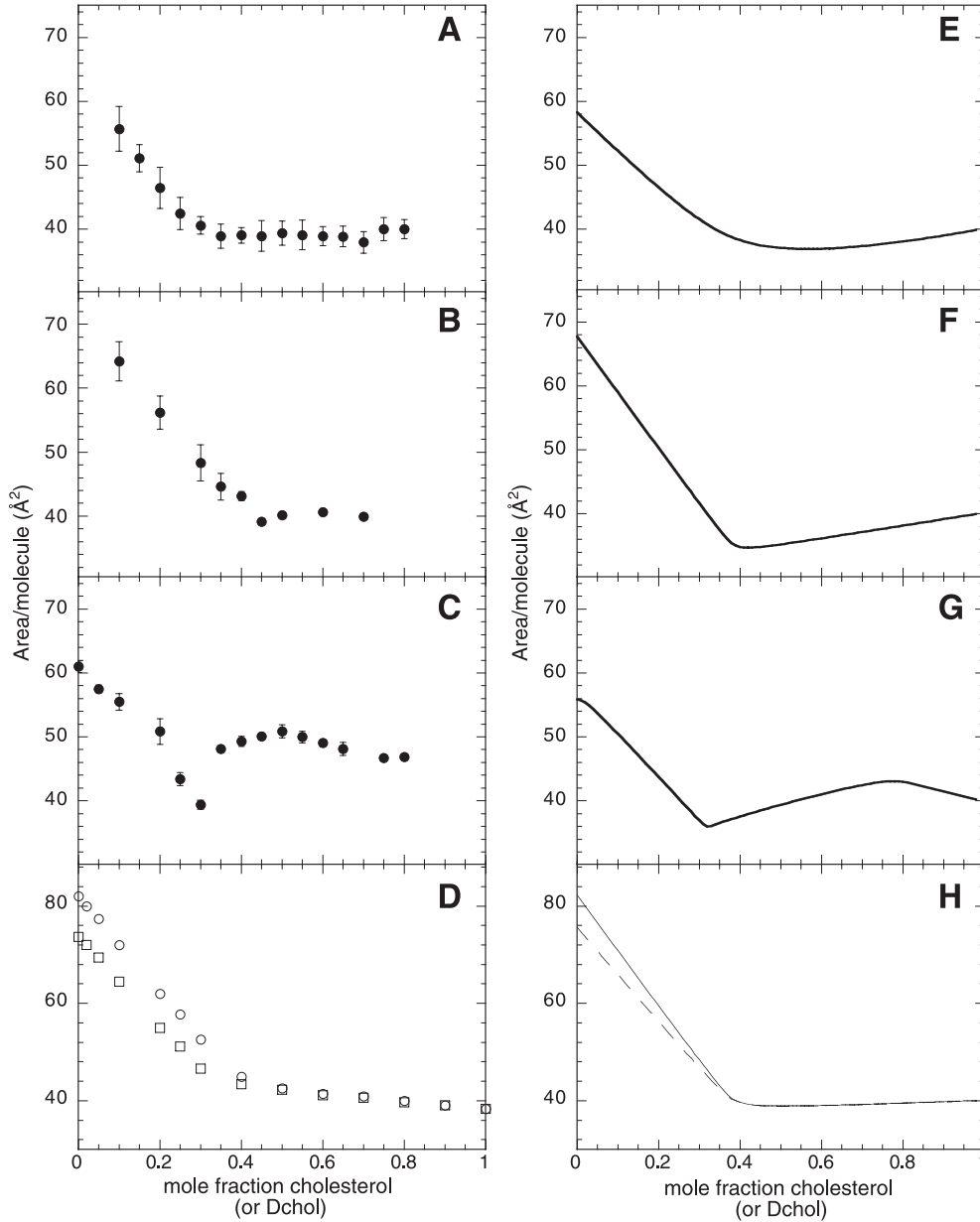


Fig. 5. Experimental average areas as a function of Dchol (or Chol) composition are shown in (A–D). All of the measurements are at room temperature, and at pressures where no phase separations are observed. (A) Mixture of DMPC and Dchol at a surface pressure of 20 dyn/cm. (B) Mixture of Dchol and a 1:1 ratio of DMPC/DPPC at a surface pressure of 20 dyn/cm. (C) Mixture of Chol and SM at a surface pressure of 22 dyn/cm. (D) Mixture of Chol and DPPC at surface pressures of 5 dyn/cm (circles) and 10 dyn/cm (squares). These data are derived from pressure–area isotherms given in Ref. [30]. Calculated average areas as a function of Dchol (or Chol) composition using a regular solution model involving repulsive interactions and where the components react to form a complex are shown in (E–H). The abbreviations C, P, and X are used for cholesterol, phospholipid, and complex, respectively. See Ref. [32] for a detailed discussion of the parameters. (E)  $\pi=20$  dyn/cm,  $q=2$ ,  $p=3$ ,  $n=1$ ,  $\bar{K}=0.9$ ,  $A_C=40$  Å<sup>2</sup>,  $A_X=(q+p)$  40 Å<sup>2</sup>,  $A_P=70(1-\kappa\pi)$  Å<sup>2</sup>, where  $\kappa=0.008$  cm/dyn,  $\pi_{PC}=10$  dyn/cm,  $\pi_{CX}=10$  dyn/cm,  $\pi_{PX}=5$  dyn/cm,  $a'_{PC}=a'_{CX}=a'_{PX}=-1/25$  cm/dyn. (F)  $\pi=20$  dyn/cm,  $q=2$ ,  $p=3$ ,  $n=5$ ,  $\bar{K}=5$ ,  $A_C=40$  Å<sup>2</sup>,  $A_X=(q+p)$  35 Å<sup>2</sup>,  $A_P=70(1-\kappa\pi)$  Å<sup>2</sup> where  $\kappa=0.001$  cm/dyn,  $\pi_{PC}=20$  dyn/cm,  $\pi_{CX}=10$  dyn/cm,  $\pi_{PX}=5$  dyn/cm. (G)  $\pi=25$  dyn/cm,  $q=1$ ,  $p=2$ ,  $n=10$ ,  $\bar{K}=1$ ,  $A_C=40$  Å<sup>2</sup>,  $A_X=(q+p)$  35 Å<sup>2</sup>,  $A_P=70(1-\kappa\pi)$  Å<sup>2</sup> where  $\kappa=0.008$  cm/dyn,  $\pi_{PC}=21$  dyn/cm,  $\pi_{CX}=22$  dyn/cm,  $\pi_{PX}=5$  dyn/cm,  $a'_{PC}=a'_{CX}=a'_{PX}=-1/25$  cm/dyn. (H)  $\pi=5$  dyn/cm (solid) and 10 dyn/cm (dashed),  $q=2$ ,  $p=3$ ,  $n=1$ ,  $\bar{K}=2$ ,  $A_C=40$  Å<sup>2</sup>,  $A_X=(q+p)$  40 Å<sup>2</sup>,  $A_P=90(1-\kappa\pi)$  Å<sup>2</sup> where  $\kappa=0.015$  cm/dyn,  $\pi_{PC}=20$  dyn/cm,  $\pi_{CX}=10$  dyn/cm,  $\pi_{PX}=5$  dyn/cm,  $a'_{PC}=a'_{CX}=a'_{PX}=-1/25$  cm/dyn.

two upper miscibility points have been observed in phase diagrams, sharp breaks in plots of average molecular areas vs. composition are also observed, *in each case at the same composition as the cusps in the phase diagrams* [21]. In the case of DMPC–Dchol mixtures at room temperature, the phase diagram shows only a single critical point, but the average molecular area plot shows a break in slope, although not a sharp break. As shown elsewhere, complexes must nonetheless be present in this mixture [40]. This is particularly evident when the temperature is lowered 10 °C. At this lower temperature, a pair of critical points is observed, as well as a sharp break in the average molecular area plot. Comparisons of this sort show the average molecular area plots to be sensitive indicators of complex formation.

In simulations of average area vs. composition plots using the model, three distinct qualitative behaviors are found. For weak complexes, no sharp breakpoints in the plots are seen (Fig. 5A and E). For stronger complexes, a distinct break is seen at the stoichiometric composition (Fig. 5B,D and F,H) (a breakpoint may be defined as the composition at which these plots show a large change of slope—often a change of the sign of the slope). The third type is one in which the break forms a cusp (Fig. 5C and G). The simulations involve a number of parameters, for which the corresponding analysis is too lengthy to present here. The most important of these parameters are the equilibrium constant,  $K$ , for reaction (1), and the stoichiometry parameters,  $p$ ,  $q$  and  $n$ . The molecular areas of phospholipid and cholesterol are obtained directly from experimental data. When the breakpoints in area vs. composition plots are sharp, the average molecular area of the complex can be easily estimated. The thermodynamic “repulsions” that give rise to liquid–liquid immiscibilities sometimes have a significant effect on the shapes of the area vs. composition plots even at the higher pressures where there is no liquid–liquid immiscibility. Two of the three repulsion terms (P–X and C–X) are derived directly from the critical pressures in the phase diagrams. The repulsions do not significantly affect the position of the cusps or breakpoints. Here, we give only a brief discussion of the more chemically important parameters used in the simulations.

The equilibrium constant  $K$  for reaction (1) depends on monolayer pressure. It is convenient to express this constant in terms of a reduced constant  $\bar{K}$ , where

$$K = \bar{K}^{np} \quad (2)$$

The reduced equilibrium constant is useful in that  $-kT \ln \bar{K}$  gives the free energy of complex formation per molecule of phospholipid in the complex. This constant depends on the monolayer pressure through the equation

$$\bar{K} = \bar{K}_0 \exp[-\pi \Delta \bar{A} / kT] \quad (3)$$

Here  $\Delta \bar{A} = \Delta A_0(1 - \kappa\pi)/np$ , and  $\Delta A_0$  is the change in molecular area that takes place when  $nq$  molecules of cholesterol

react with  $np$  molecules of phospholipid to produce a molecule of  $C_{nq}P_{np}$ , all at zero monolayer pressure. The quantity  $\Delta \bar{A}$  is the change in area associated with this reaction per phospholipid molecule, at pressure  $\pi$ , where  $\kappa$  is the compressibility of the phospholipid. The reduced quantities  $\bar{K}$  and  $\Delta \bar{A}$  are useful for comparing calculations involving different values of  $n$  and  $p$ , and for comparing thermochemical data for monolayers and bilayers.

The legend to Fig. 5 gives numerical values of the parameters used for the simulations shown. The immiscibility parameters given in this legend are defined elsewhere [32]. It is generally observed that when the breakpoints in these plots are sharp, the average molecular area at the complex stoichiometry is approximately equal to the molecular area of pure cholesterol (at the same pressure). This is consistent with the equality of the partial molar areas at the equivalence point. A tangent at the equivalence point determines the difference in the partial molar areas. This tangent often has zero slope at the equivalence point. Thus the quantity  $\Delta \bar{A}$  is essentially the change in area of a phospholipid molecule associated with the formation of a complex, and is typically about  $-30 \text{ \AA}^2$  at pressures of 20 dyn/cm, for example. Due to area contraction in the reaction, complexes are stabilized by increases of pressure. The rate of increase of stabilization is reduced with increasing pressure due to compression of the phospholipid molecules not in the complex. That is, the area contraction is smaller at the higher pressures. The complexes themselves and cholesterol are relatively incompressible, and their compressibility is neglected (see Fig. 5D). The compressibility of phospholipids at pressures corresponding to the “liquid expanded” phase are of the order of magnitude 0.001–0.015 cm/dyn [30,41]. The area parameters are easily estimated from monolayer areas.

Unfortunately, there appears to be no simple method to determine the equilibrium constants for the reactions of complex formation, or to determine values of  $n$ . These parameters are estimated by fitting both phase diagrams and average area plots to the model. For an area plot in which there is a sharp break in slope, and low average area at equivalence, all simulations imply nearly complete reaction. The equilibrium constants and values of  $n$  given in the legend to Fig. 5 are semi-quantitatively consistent with average area plots, and observed phase diagrams (in previous work, the compressibility term was not included, so some modification of earlier estimates of these parameters may be desirable). When the equilibrium constants  $\bar{K}$  are of the order of magnitude 1,  $|\Delta \bar{H}|$  is large compared to  $|\Delta \bar{F}|$ , and  $\Delta \bar{S} \approx \Delta \bar{H}/T$ , a relationship similar to the freezing of a liquid, at equilibrium (recall that  $\Delta \bar{F} = -RT \ln \bar{K}$ ). For the DMPC–Dchol mixture,  $\Delta \bar{S} \approx -30 \text{ eu}$  [40].

### 2.3. Condensed complexes—a separate liquid phase or not?

At the lower monolayer pressures, the third phase X is largely condensed complex. According to the model, at the

higher pressures, the phase X becomes miscible with the other phases. P and C likewise become miscible with one another, so the membrane forms a homogeneous liquid phase. The model calculations imply that the complexes remain at the higher pressure. Do they? The data on average molecular areas at the higher pressures cited above (where there are no immiscibilities) show clearly that these complexes are indeed present even when not forming a separate phase. As discussed below, the presence of the condensed complexes in the homogeneous phase at the higher pressures has also been demonstrated in two additional experiments, one measuring the “chemical activity” of cholesterol, and the other measuring the response to an electric field gradient.

#### 2.4. Complexes affect the chemical activity of cholesterol

A classic terminology for chemical activity is *fugacity*, meaning “tendency to flee.” It has been pointed out that the tendency of cholesterol to leave a membrane should be related to its chemical activity [21]. For example, in an ideal two-dimensional membrane, the flux of cholesterol molecules leaving the membrane should be proportional to the mole fraction of cholesterol in the membrane. In the model calculations, this flux is reduced by the formation of complexes and is also affected by the intermolecular interactions leading to immiscibility. In this general case, the flux is expected to be proportional to the chemical activity of cholesterol. The probability per unit time that an individual molecule of cholesterol leave the membrane is the chemical activity divided by the mole fraction of cholesterol. Thus, as a rough first approximation, the activity coefficient of cholesterol can be thought of as being proportional to the fraction of the time a cholesterol molecule is free, not complexed to phospholipid. When the complex is stable and phospholipid is in excess, cholesterol is mostly tied up as a complex, so that both the activity and activity coefficients are small. When cholesterol is in excess, some cholesterol cannot be tied up in complex, so both the activity and activity coefficients are higher. Both activities and activity coefficients as a function of composition are readily derived from the model.

Measurements of cholesterol desorption rates from monolayers to  $\beta$ -cyclodextrin can be analyzed in terms of kinetic first-order rate constants. It has been found in both theory and experiment that the chemical activity (and activity coefficient) increases rapidly with increasing cholesterol concentration at the equivalence point. Illustrative data are shown in Fig. 6, for the case of 2:1 DMPS:DMPC–Dchol [21]. The observed release rates are given in Fig. 6B, and theoretical chemical activities and activity coefficients are given in Fig. 6C. The theoretical calculations are based on the thermodynamic parameters used to model the molecular area data for the same binary mixture. These parameters also model the experimental phase diagram for this mixture (Fig. 4A). Fig. 6A gives a schematic repre-

sentation of a monolayer containing free cholesterol, and free phospholipid together with a cholesterol–phospholipid complex.

#### 2.5. Dissociation of complexes with an electric field

Molecules at the air–water interface give rise to a surface potential due to components of molecular dipole moments perpendicular to the surface. In the case of charged monolayers, the electrostatic double layer can also contribute to this potential. In cholesterol–phospholipid monolayers, the strength of these dipoles is of the order of magnitude 1 D/100 Å<sup>2</sup> [20] (there is no reliable method for measuring dipole densities for a single phase. In Ref. [20], dipole density differences were measured between coexisting liquid phases and in this respect are relevant to the present discussion). In our experiments, the sense of this dipole density is positive up, negative down, as illustrated in Fig. 7A. A significant contribution to this dipole density is thought to arise from the terminal methyl groups. Surface dipoles such as those that could arise from terminal methyl groups are not screened by the aqueous subphase; in fact, by classical electrostatic theory, the subphase dielectric augments these dipole moments. In molecular dynamics simulations [42], it has been proposed that the orientation of surface water molecules makes an important contribution to surface potentials in phospholipid membranes. In any event, the molecular origin of surface potentials is not important for the discussion in this review.

It is possible to apply an electric field to a monolayer at the air–water interface [24]. A schematic of the experimental setup is shown in Fig. 7A. The effect of this field is to stabilize, or destabilize complexes depending on (a) the direction of the field, (b) the sign of the dipole moment, and (c) whether complex formation increases or decreases the dipole density in the monolayer. Experimental and theoretical analysis confirms this expectation, providing compelling evidence that these complexes are present in the homogeneous phase at higher pressures [37]. Complex formation increases the dipole density of the monolayer, so that an applied field tends to destabilize the complex, when the field direction is plus-to-minus towards the monolayer.

The quantitative analysis of this field effect is given elsewhere [37]. Suffice it to say here that the field applied was non-uniform, as illustrated in Fig. 7. At distances close to the electrode, the large field gradient gives rise to separations into three distinct phases, a complex-rich phase, a cholesterol-rich phase, and a phospholipid-rich phase, all arising from a monolayer that was homogeneous in the absence of the field. In the epifluorescence micrographs of Fig. 7B and C the camera looks down on the electrode. Moving away from the electrode in the presence of the field, the coexisting phases are phospholipid (bright), cholesterol (dark) and complex (bright). Note that the phospholipid phase forms small bright circular domains. The cholesterol-

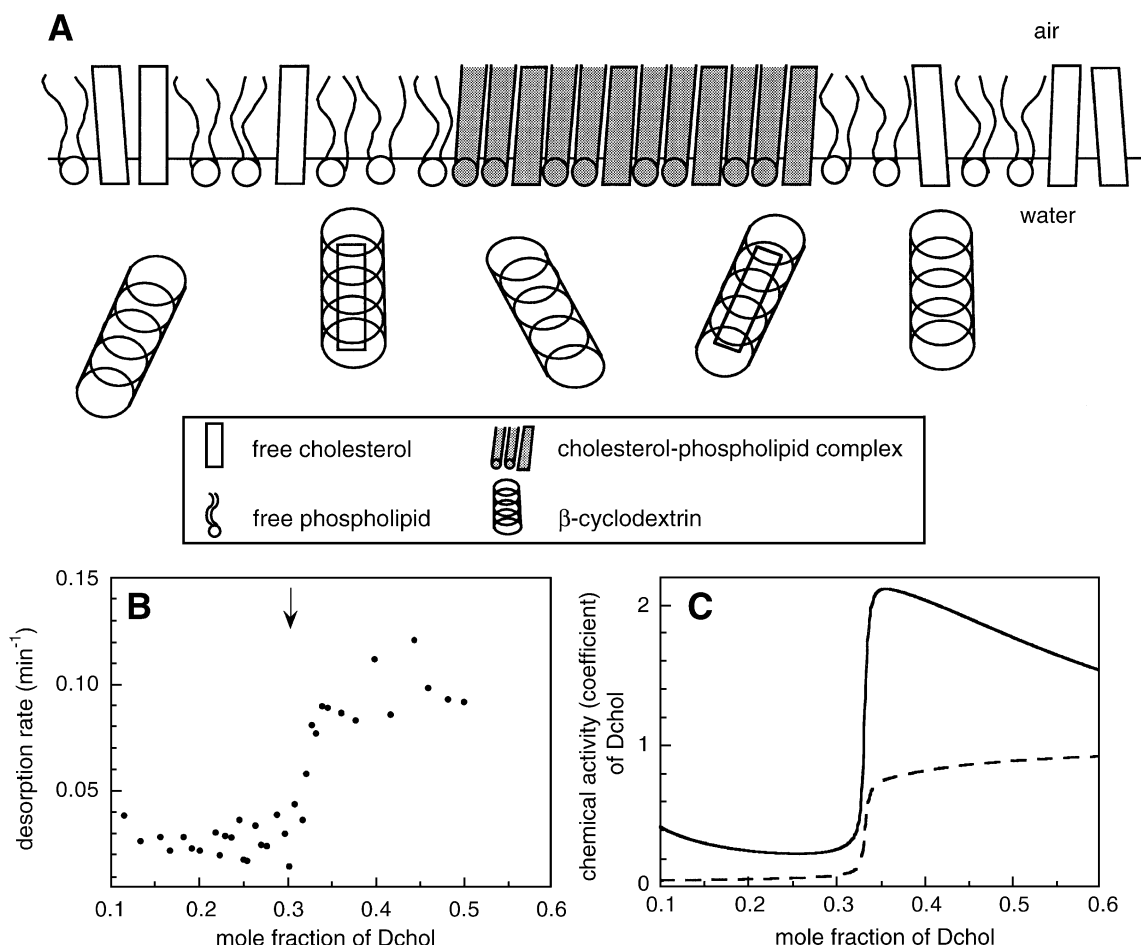


Fig. 6. Detection of condensed complexes in homogeneous membranes at high pressures by measuring the chemical activity coefficient of cholesterol (or Dchol). (A) Schematic of a lipid monolayer containing molecules of cholesterol (or Dchol), phospholipid, and condensed complex. The subphase contains 1–2 mM of  $\beta$ -cyclodextrin which selectively desorbs cholesterol (or Dchol) from the air–water interface. The desorption rate is proportional to the chemical activity of cholesterol. (B) Desorption rate constants for Dchol release from single phase, homogeneous membranes to  $\beta$ -cyclodextrin. The lipid monolayer starts off with a composition of 50 mol% Dchol and 50 mol% of a 2:1 molar mixture of DMPS:DMPC (see Fig. 4A for phase diagram) at a surface pressure of 22 dyn/cm (above the critical pressures). The sharp break in the desorption rate constants occurs at a Dchol composition corresponding to the equivalence point (arrow at 30 mol% Dchol). (C) Theoretical cholesterol chemical activity (dashed line) and activity coefficient (solid line) as a function of cholesterol concentration in a single-phase, homogeneous membrane. These quantities are calculated using the same parameters as those listed for Fig. 5G, and shows a sharp jump at the equivalence point.

rich phase is continuous and dark. Molecules of phospholipid, cholesterol and complex in the presence of a field gradient are drawn schematically in Fig. 7A. For all mixtures studied, the electric field effect is only observed for monolayer compositions within a few mole percent of the equivalence point. At this composition, the concentration of complex is highest, and the system most susceptible to the field effect.

## 2.6. Membrane properties at the equivalence point

As noted above, when the equilibrium of reaction (1) lies far to the right, then many membrane properties are expected to change rapidly near the equivalence point. This is reflected in the phase diagrams showing complex formation, as well as in the chemical activity, average molecular area and electric field susceptibility. More generally, the

relative chemical potentials of cholesterol and phospholipid change sign as one passes through the equivalence point. The two chemical potentials are therefore equal at the equivalence point. The partial molar areas of cholesterol and phospholipid are also often equal to one another at this point (40 Å<sup>2</sup>/molecule). As discussed later, this has implications for the molecular structure of complexes.

## 2.7. Thermochemistry—large exothermic heat of reaction

There have been many scanning calorimetric studies of binary mixtures of phospholipids and cholesterol in bilayer membranes [4,13]. Binary mixtures of saturated phosphatidylcholines and cholesterol have been studied most extensively [43,44]. These mixtures are particularly interesting because in addition to the chain melting transition characteristic of the pure phospholipid, the mixtures show an addi-



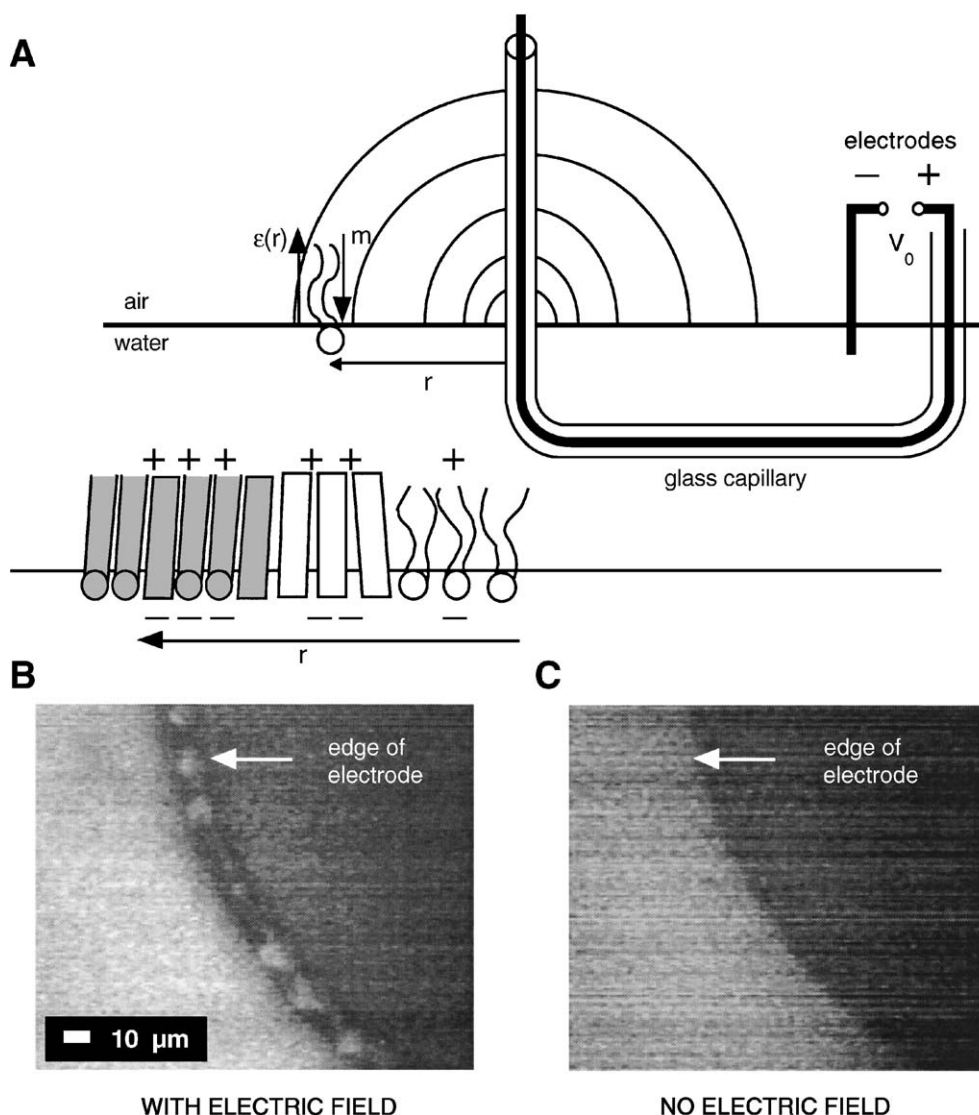


Fig. 7. Dissociation of condensed complexes in homogeneous membranes at elevated pressures using an inhomogeneous electric field. (A) Schematic for the experimental setup. An inhomogeneous electric field is generated at the air–water interface by applying a potential  $V_0$  to an insulated tungsten electrode shown in boldface (radius =  $6\ \mu\text{m}$  at the tip). The electric field strength perpendicular to the surface of the interface is denoted  $\varepsilon(r)$ . In monolayers, lipid molecules have dipole moments ( $m$ ) which are perpendicular to the air–water interface. An applied electric field in the proper direction can destabilize the complex (which has the highest dipole density) and under some conditions, result in a field-induced phase separation near the electrode. This is shown schematically in the bottom panel where there is a complex-free zone near the electrode in which a phospholipid-rich phase (closest to the electrode) coexists with a cholesterol-rich phase (use same key as in Fig. 6A). (B) Epifluorescence micrograph of a lipid monolayer consisting of DMPS, DMPC, and Dchol in the presence of an inhomogeneous electric field ( $V_0 = 150$  volts). The lipid monolayer contains 21.6 mol% DMPC, 43.2 mol% DMPS, 35 mol% Dchol, and 0.2% TR-DHPE. The surface pressure is 21 dyn/cm, well above the critical pressures for the system (see Fig. 4A for the phase diagram), and a field-induced phase separation can be seen in a narrow band around the electrode. (C) Epifluorescence micrograph of the same lipid monolayer as in B when there is no electric field. The monolayer appears uniformly gray around the electrode (as one would expect from the phase diagram of Fig. 4A).

tional broad transition. Recent work has analyzed this broad transition in terms of the thermal dissociation of condensed complexes [45]. In this analysis, a rather large cooperativity parameter,  $n = 12$ , provided a better fit to the data than smaller values for  $n$ . It should not be surprising to find that cooperativity for complex formation is stronger in bilayers than in monolayers. The deduced exothermic heats of reaction are surprisingly large, ranging from  $-6$  to  $-20$  kcal/mol of phospholipid for phospholipids with 14–20 carbon atoms in each saturated chain.

The large heats of reaction for complex formation inferred from the bilayer calorimetry correspond to a large temperature dependence for complex formation. This led to a study of the temperature dependence of the phase diagram of monolayer mixtures of Dchol and DMPC. At room temperature ( $23\ ^\circ\text{C}$ ) a binary mixture of these lipids shows only weak evidence of complex formation, whereas at lower temperatures ( $13\ ^\circ\text{C}$ ) evidence for complex formation is unambiguous. The heat of reaction inferred from the monolayer phase diagram and chemical activity coefficient meas-

urement is  $-9$  kcal/mol of phospholipid. This corresponds to  $-27$  kcal/mol for the apparent complex stoichiometry  $C_2P_3$  [40]. Most of the monolayer experiments discussed here were carried out at  $23^\circ\text{C}$ .

### 2.8. Multicomponent complexes—different phospholipids in one complex

Multicomponent mixtures of phospholipids and cholesterol often behave as though they are pseudo-binary mixtures. These are mixtures for which the ratios of the mole fractions of phospholipids to one another remain fixed as the cholesterol concentration is changed. Plots of phase boundaries vs. cholesterol concentration yield phase diagrams similar to those found for binary mixtures. An example is shown in Fig. 4A. A significant finding is that these diagrams typically show only a single sharp cusp, suggesting the presence of only one complex stoichiometry. That is, there is a single equivalence point. This is confirmed by cholesterol desorption (chemical activity) experiments (see Fig. 6B). This shows that different phospholipids participate in forming a single complex.

### 2.9. The size, structure, and lifetimes of condensed complexes

As indicated earlier, one cannot expect to find long-range molecular order in a liquid membrane. On the other hand, complex formation implies molecular order. We suggest that this order is short-range with close packing of phospholipid and cholesterol molecules. The complexes themselves must undergo relatively free translational motion, rotational motion, and/or reptation. The complexes are also likely to have relatively short half-lives, for example, between a microsecond and a millisecond. When a membrane is largely composed of complex, the boundaries between complexes must be disordered. That is, the molecular order is short-range ( $\sim 3$ – $10$  intermolecular lengths or  $30$ – $100$  Å). Ultimately, it may be possible to infer complex lifetimes from NMR data. For example, Vist and Davis [16] have used broadening of deuterium NMR signals to infer liquid–liquid phase separations in cholesterol–dipalmitoylphosphatidylcholine (DPPC) mixtures. However, complex formation might also yield line broadening if the complex lifetimes are comparable to or exceed the typical deuterium NMR time-scale ( $\sim 10$  μs).

The close packing of molecules is suggested by the equality of the partial molar areas of cholesterol and phospholipid at the equivalence point in binary mixtures, mentioned above. The membrane area occupied by a cholesterol molecule is about  $37$  Å<sup>2</sup> in a compressed cholesterol monolayer. This molecule has a rigid molecular ring system and is relatively incompressible at this molecular area [30,46]. Phospholipid molecules in the liquid phase are highly compressible at the pressures used for monolayer studies. In the compressed or gel state having largely *trans*

fatty acid chains, phospholipids require surface areas of about  $45$  Å<sup>2</sup> [47]. In the crystalline or highly compressed monolayer states of some phospholipids, these areas can be even less, of the order of  $40$  Å<sup>2</sup> [46,48]. As inferred from monolayer data, the average molecular areas in the more stable complexes are sometimes somewhat less than  $40$  Å<sup>2</sup> (an average molecular area of  $44$  Å<sup>2</sup> was estimated for the red cell membrane, which contains about  $42$  mol% cholesterol [49]). Thus, in the complexes, the chains must be largely in the all *trans* conformation, and the molecules are likely to be closely packed. Consequently, membrane regions composed of condensed complexes are likely to be thicker than other regions. It has been observed that the *sn* 1 fatty acid chain of phospholipids appears to be more significant for area condensation (due to cholesterol) than the *sn* 2 chain [36,39,50]. Thus, it is unlikely that the two chains of phospholipids occupy equivalent positions in the complexes [36].

Plots of average molecular area vs. composition provided some of the earliest evidence suggesting the formation of phospholipid–cholesterol complexes. This early work is summarized by Phillips [38]. It should be noted that in the early work, liquid–liquid immiscibility was only suspected. Here we view various aspects of complex formation under conditions where the pressure is high enough that there is no immiscibility.

Consider first the simplest possible case. (1) A complex  $CP_2$  has high stability. In this event, when cholesterol is added to a phospholipid membrane,  $CP_2$  is formed and the area of the membrane accordingly decreases until the equivalence point is reached when the mole fraction of cholesterol is  $0.33$ . In this regime, the area of the membrane is a linear function of the mole fraction of cholesterol. When more cholesterol is added, beyond the equivalence point, the cholesterol simply mixes with the complexes (or forms a separate phase), and there is relatively little additional change in average molecular area.

In case (2),  $CP_2$  molecules are not formed but molecules such as  $C_3P_6$  are formed, where  $n = 3$ . The evidence for such larger complexes comes from simulations of the phase diagrams, as well as electric field effects, and the thermochemistry of bilayers, where values of  $n$  substantially above  $1$  are required to fit experimental data [37,45]. Also, complexes having more than one molecule of cholesterol are implied by some phase diagram cusp points, and break-points in area plots. One example is  $C_2P_3$ , illustrated in Fig. 5B,F, and D,H (also, see Ref. [36]).

The above considerations are made somewhat complicated by the immiscibility parameters in the model. With these parameters, complexes “feel” the presence of other molecules (the liquid composition) and this can lead to a deviation of the average area vs. cholesterol composition plots from linearity above and below the equivalence point. This effect contributes to the marked non-linear regions seen in Fig. 5C,G, but not at very low cholesterol concentrations. The parameters used in Fig. 5 were picked to simulate phase

diagrams (for example Fig. 3A), molecular areas (Fig. 5C), and chemical activity coefficient measurements (Fig. 6B). This triple fitting severely limits the choices for most of the parameters.

A third limiting case, case (3), has been discussed theoretically [51]. In this case, simple complexes such as  $CP_2$  are formed, but they can oligomerize to form an infinite series of larger complexes, such as  $C_nP_{2n}$ . In this case, linearity of the area plots appears naturally when, as expected, these various complexes have the same average molecular density. As the case  $n \rightarrow \infty$  is approached, the area vs. composition plots can be ideal at low concentrations of cholesterol (and phospholipid), and then deviate at higher concentrations. This limiting behavior has not been seen experimentally in monolayers. The data shown in Fig. 5C and G for egg-sphingomyelin–Dchol are modeled using  $n = 10$ .

Modeling of experimental monolayer data in terms of complexes with a small number of discrete values of  $n$  has not been attempted (modeling of mixtures with multiple complexes having different values of  $p$  and  $q$  has been carried out [52]). Although this extension of the model is physically plausible, it is replete with latent complications. These include the possibilities of a composition as well as a pressure dependence of  $n$ .

The disorder associated with chain motion is largest for the shorter as well as unsaturated fatty acid chains [48]. In our work, it appears that higher proportions of cholesterol are required to suppress these motions at the equivalence point. That is, it has been a general observation in our work that the cholesterol composition at the equivalence point is largest when the phospholipid fatty acid chains are short or are dissimilar in chain length [36]. The stoichiometric compositions vary from 25% to 50% cholesterol.

The above discussion leads to a picture in which condensed complexes have finite sizes, and contain closely packed molecules. All of these molecules are chiral. It is therefore plausible that the complexes themselves have chiral shapes (see Ref. [53] for chiral solid domain shapes in monolayers). Complexes containing as many as 100 closely packed molecules might be detectable with synchrotron X-ray scattering [48,54]. Speculative qualitative sketches of ordered molecules are given in Figs. 6A and 7A.

### 2.10. Superlattice models

A number of investigators have proposed the formation of *superlattice structures* in bilayer mixtures of phospholipid and cholesterol [10–12,55]. Their work is related to the observation of non-monotonic variations in the physical properties of bilayers as a function of cholesterol concentration. These variations might possibly be interpreted as the formation of complexes with different stoichiometries [52]. We find no evidence for multiple complexes in monolayers, although weak complexes might escape detection. Of course monolayer studies obviously do not preclude their presence in bilayers.

It may be noted that in a number of lattice models of cholesterol–phospholipid mixtures, it is assumed that a cholesterol molecule occupies the same lateral area as does a single chain of a phospholipid. As noted above, we believe that, on the contrary, it is cholesterol and entire phospholipid molecules that occupy equal lateral areas at compositions corresponding to condensed complexes.

## 3. Monolayers, bilayers and cell membranes

### 3.1. Phase separation in bilayers

An early attack on the monolayer vs. bilayer relationship problem was made by Tajima [5] and Tajima and Gershfeld [56]. These investigators used monolayer surface pressures to infer the presence of 1:2 cholesterol–phospholipid complexes in bilayers in the subphase. Under conditions of chemical equilibrium, the chemical potentials of the various components in the monolayer and bilayer membranes should be the same, so monolayer properties should reflect bilayer properties. An extensive review of experimental as well as theoretical aspects of the relation between the physical chemistry of monolayers and bilayers has been given by Marsh [41] (also see Ref. [47]). An important conclusion reached in Ref. [41] is that at pressures in the range 30–35 dyn/cm monolayers have properties that closely mimic the properties of bilayers. The reported monolayer two-phase regions are generally found at pressures lower than this range. However, the electric field, cholesterol desorption, and molecular area measurements show the expected persistence of complexes at higher pressures, certainly as high as 20–25 dyn/cm [21,37].

There are a number of early experimental studies postulating liquid–liquid phase separations in cholesterol–phosphatidylcholine bilayer mixtures [15,16]. Such liquid–liquid phase separations have recently been observed in cholesterol–phospholipid bilayer mixtures [57–59]. The domains reported have a striking similarity to those seen in monolayers. Of the two phases observed, the phase with the higher cholesterol concentration is likely to be the condensed complex phase. In these symmetrical bilayers, condensed complexes on one side of the bilayer are paired with complexes on the other side. As discussed later, we have recently discovered a third two-phase region ( $\gamma$ ) in monolayers. We believe that this  $\gamma$  two-phase region corresponds to the two-phase regions in bilayers.

Determination of the phase diagrams for mixtures of lipids in bilayers is important but potentially more difficult than in monolayers. Fundamental problems contribute to this. In bilayers, phase separations may be transmembrane as well as lateral. Also, bilayer mixtures may undergo line tension-mediated fission, leading to vesicles with different compositions. For a theoretical discussion of this mechanism of vesicle formation, see the chapter by Lipowsky and Sackmann in Ref. [60].

### 3.2. The liquid ordered phase, and condensed complexes

In 1987, Ipsen et al. [17] introduced the term *liquid ordered phase* to describe qualitative as well as quantitative aspects of mixtures of cholesterol and phospholipids. This descriptive term has been adopted by many investigators in the field of membrane biology. The term *liquid ordered* derives from the cholesterol-mediated ordering of the fatty acid chains of phospholipids that has been inferred using many techniques [13]. Ipsen et al. used a clever mean field thermodynamic model to describe the formation of immiscible liquid phases in cholesterol–phospholipid mixtures. Just as in the condensed complex model, three components are considered. In their case, the components were cholesterol, phospholipid molecules with ordered chains, and phospholipids with disordered chains. The important difference in the models arises from the fact that Ipsen et al. treated all the interactions between the components by the approximation of regular solution theory. In particular, intermolecular interaction energies were treated as quadratic functions of concentrations. If these investigators had instead assumed that cholesterol and phospholipid molecules with ordered chains underwent a reaction to form complexes, then their model would be equivalent to ours. The important difference in treating intermolecular interactions in terms of a chemical reaction formalism (complex formation) relative to a power series expansion can be seen by comparing the results of Corrales and Wheeler [33] with those of Okamoto [61]. Both approaches give pairs of upper miscibility critical points, but the cusp in the phase diagram can be much sharper in the presence of a chemical reaction (as observed experimentally). The term liquid ordered phase is certainly descriptive of a phase formed by condensed complexes, but is also descriptive of a cholesterol-rich phase in equilibrium with the condensed complex phase, as well as a cholesterol-rich phase in equilibrium with a phospholipid-rich phase.

In recent work, the present authors have found that mixtures containing dimyristoylphosphatidylserine (DMPS), ganglioside G<sub>M1</sub>, and cholesterol show *three* miscibility critical points [62]. Two upper miscibility critical points and the corresponding  $\alpha$  and  $\beta$  two-phase regions are closely similar to those described in Figs. 3 and 4, and elsewhere [32,36]. The third two-phase region,  $\gamma$ , has a lower miscibility critical point, and is roughly the mirror image of the  $\alpha$  two-phase region. We suggest that this  $\gamma$  two-phase region is to be compared with the two-phase region of Ipsen et al. describing the *liquid ordered phase* and the *liquid disordered phase*. In our work, the  $\gamma$  as well as the  $\alpha$  and  $\beta$  two-phase regions conform nicely to the condensed complex model, with phase boundaries sharply delimited by the stoichiometric composition. More generally, it is likely that the  $\gamma$  two-phase region in monolayers will be found to correspond most closely to regions of liquid–liquid immiscibility in bilayers.

Mouritsen et al. [63,64] have also developed a microscopic molecular model for cholesterol–phospholipid mix-

tures, guided in part by calorimetric and NMR data on bilayers. In principle, such calculations are sufficiently general that they should include condensed complexes as a special case. However, these calculations have not yet yielded any sharp change of properties at compositions corresponding to stoichiometric points. It should certainly be possible to introduce this feature into a microscopic molecular model with a suitable choice of interaction parameters.

### 3.3. Rafts and condensed complexes

There is now a large literature postulating the existence of specialized regions in cell membranes referred to as *rafts* [65]. These regions are said to contain selected proteins, to be enriched in cholesterol, sphingomyelin and other saturated long chain phospholipids, and to be important for a variety of cellular functions [66–71]. Rafts have sometimes been identified as distinct domains in cell membranes, and/or as regions in which membrane components exhibit reduced diffusion [72,73]. Rafts have also been identified with detergent-resistant membrane fractions [66,67]. Condensed complexes and rafts would then appear to be similar to one another in terms of lipid composition [74].

It is of course possible in principle to model protein–lipid interactions in terms of complexes [75,76]. It is physically plausible that some proteins interact with condensed complexes more strongly than with lipids not in complexes. A number of effects could contribute to this specificity, including hydrophobic matching related to bilayer thickness [69]. Also, as in liquid crystals, neighboring molecules are likely to have similar order parameters. Protein molecules are relatively rigid and should have large order parameters, and so should neighboring lipid molecules. The molecular environment of some proteins could then be specifically condensed complex. Of particular interest is the theoretical possibility of proteins that are asymmetric with respect to their lipid interactions [77]. Such proteins might stabilize lipid regions of differing composition, and play a role in domain and vesicle formation. As noted above, in the absence of proteins, the complexes themselves may have chiral shapes. The associated molecular anisotropy could be relevant to lipid–protein interaction. It is interesting to note that small chiral domains have recently been proposed to be involved in vesicle budding [78].

### 3.4. Condensed complexes in cell membranes

It is likely that condensed complexes are present in the plasma membranes of animal cells in view of the reported relatively high concentrations of cholesterol, sphingomyelin, and other saturated long-chain phospholipids. Phosphatidylserines and phosphatidylethanolamines are typically found on the inner leaflet of the plasma membrane [69]. These phospholipids also form condensed complexes with cholesterol [36]. It is probable that complexes on one side of



the membrane are paired with complexes on the other side (again, as in liquid crystals, neighboring molecules generally have similar order parameters). As noted above, the complexes need not form a separate phase. They may be simply dissolved in the liquid membrane. Alternatively, an entire membrane might be mostly liquid complex. Complexes forming a second liquid phase in a single membrane should be more easily characterized and identified experimentally. However, to our knowledge, a liquid–liquid phase boundary in a biological membrane under physiological conditions has not been demonstrated. The line tension associated with liquid–liquid immiscibility in lipid monolayers must apply to lipid bilayers as well [20]. This tension represents a high local energy density and the liquid–liquid interface would be a non-specific trap for many different substances. On the other hand, it is plausible to conjecture a liquid–liquid interface stabilized by specific proteins or special lipids. There is a large literature dealing with lipid–protein interactions as studied using paramagnetic resonance spin label spectroscopy [75,76,79,80]. One unambiguous result from these studies is that the motional freedom of labeled phospholipids adjacent to proteins is strongly suppressed. Thus condensed complexes also having relatively immobilized lipid chains are likely to be associated with some membrane proteins. In this connection, see Refs. [81,82].

Many authors have discussed the fact that different membranes within a given cell have different lipid compositions [69,83,84]. The lipids in distinct membranes such as the plasma membrane and the endoplasmic reticulum (ER) membrane can be thought of as forming separate liquid phases. It is plausible that the chemical activity of cholesterol in the ER is roughly equal to the chemical activity of cholesterol in the plasma membrane. This situation can arise when the activity of cholesterol in the plasma membrane is low because most of the cholesterol is tied up in complexes, and when the chemical activity of cholesterol in the ER is low because the total concentration is low (the low cholesterol concentration in the ER would be related to its low affinity for cholesterol. The ER has unsaturated phospholipids that presumably do not form strong complexes). One may postulate that fluxes of cholesterol in cells move down a gradient of chemical potential, from ER (source) to plasma membrane (sink) or vice versa, depending on variations in membrane compositions. This of course would doubtless require associated proteins for sensing and translocation [85,86]. For an overview of lipid transport between membranes in cells, see Ref. [69]. Observations from cell biology suggesting to us a possible regulatory role for complexes can be found in Refs. [87–90].

As noted above, studies of multicomponent mixtures imply that different phospholipids may participate in a single condensed complex with cholesterol. One may consider the possibility that plasma membranes normally have compositions corresponding to an equivalence point (see Ref. [91]). In this circumstance, the chemical activities of

cholesterol and phospholipids would be sensitive to membrane composition. This composition-dependent switch in the chemical activity of cholesterol could serve a regulatory function [88,89]. Also, the lipids in the membrane could then be poised for protein controlled domain formation and lipid phase separation (vesicle formation).

### 3.5. Lateral diffusion

It is difficult to study condensed complexes in monolayers and bilayers using measurements of lateral diffusion. The following factors are significant. The molecules in a condensed complex are closely packed, so their intermolecular distances are not expected to change rapidly within the lifetime of the complex. However, the translational and rotational diffusion coefficients of the entire complex may nonetheless be quite large, though not as large as a free phospholipid molecule in a phospholipid bilayer ( $\sim 1 \mu\text{m}^2/\text{s}$ ). We estimate, on theoretical grounds, that the diffusion coefficient of an isolated complex containing 100 molecules in a phospholipid bilayer should only be on the order of one-half that of a free lipid molecule [28]. Even when the membrane approaches 100% complex the average diffusion of phospholipid molecules might remain substantial if the lifetime of the complexes is short. That is, molecules in a complex would transform rapidly into molecules not in complexes, and vice versa. Molecules not in complexes could move in interconnected defect regions, and again might also show only a factor of 2 lower diffusion coefficient.

The above theoretical speculations are consistent with the observed reduction in diffusion of a phospholipid probe incorporated in phospholipid bilayers containing variable amounts of cholesterol [92]. In this case, the diffusion coefficient was reduced by a factor of 3–5 in the vicinity of a putative stoichiometric point. Clearly, for monolayers and bilayers, any attempt to characterize condensed complexes using diffusion measurements will be a challenge. On the other hand, it is likely that some proteins may act to stabilize or confine condensed complexes, increasing their lifetimes and slowing their diffusion. In this event, chemically distinct probes may be found that distinguish regions of complex from those free of complex, in which case, distinct short-time diffusion behavior may be observed even in a macroscopically homogeneous membrane. In such cases, fluorescence resonance energy transfer may also offer the possibility of detecting molecules associated with condensed complexes [93,94].

## 4. Conclusions/summary

The condensed complex model for cholesterol–phospholipid mixtures has features in common with earlier qualitative ideas and quantitative studies. Some important features of the model are quite distinct, and have led to novel

predictions, a number of which have been verified experimentally. As an example, the jump in the chemical activity of cholesterol at the stoichiometric composition was not anticipated by earlier work. The model is quantitative yet relatively simple and intuitive. In the complex, cholesterol and phospholipid molecules occupy nearly equal areas. Thus, the complexes are likely to contain closely packed molecules and may have chiral shapes.

### Note added in proof

An unexpected aspect of the beta two-phase region has been uncovered in preliminary work with Tamara Okonogi (unpublished). The data points that define the boundaries of the beta two-phase field in Figs. 3 and 4 correspond to the disappearance of the small fluorescent domains (white in Fig. 4D) at the given pressures. Recent experiments indicate that at such points the domains do not disappear on increasing pressure. Instead the domains abruptly become darker, due to the loss of TR-DHPE to the surrounding liquid. Thus the beta two-phase regions reported by us in earlier work might extend to significantly higher pressures. This contrast inversion has not been seen in the alpha two-phase region. However, a lower miscibility critical pressure has been found in one mixture just above the alpha two-phase critical pressure, again showing the possibility of immiscibility at high monolayer pressures [62].

### Acknowledgements

We are indebted to Thomas Anderson and Marija Vrljic for many helpful discussions. This research was supported by the NIH (Grant: 5R01AI13587-27).

### References

- [1] J.B. Leathes, *Lancet* 208 (1925) 853–856.
- [2] J.B. Finean, *Experientia* 9 (1953) 17–19.
- [3] D.G. Dervichian, *Surface Science in Chemistry and Biology*, Pergamon, Oxford, 1958.
- [4] H. Hinz, J.M. Sturtevant, *J. Biol. Chem.* 247 (1972) 3697–3700.
- [5] N.L. Gershfeld, *Biophys. J.* 22 (1978) 469–488.
- [6] D. Needham, T.J. McIntosh, E. Evans, *Biochemistry* 27 (1988) 4668–4673.
- [7] J.H. Ipsen, O.G. Mouritsen, *J. Chem. Phys.* 91 (1989) 1855–1865.
- [8] J. Huang, G.W. Feigenson, *Biophys. J.* 76 (1999) 2142–2157.
- [9] M.B. Sankaram, T.E. Thompson, *Biochemistry* 29 (1990) 10676–10684.
- [10] M.M. Wang, I.P. Sugar, P.L. Chong, *Biochemistry* 37 (1998) 11797–11805.
- [11] I.P. Sugar, D. Tang, P.L. Chong, *J. Phys. Chem.* 98 (1994) 7201–7210.
- [12] J.A. Virtanen, M. Ruonala, M. Vauhkonen, P. Somerharju, *Biochemistry* 34 (1995) 11568–11581.
- [13] L. Feingold, *Cholesterol in Membrane Models*, CRC Press, Ann Arbor, 1993.
- [14] S. Subramaniam, H.M. McConnell, *J. Phys. Chem.* 91 (1987) 1715–1718.
- [15] D.J. Recktenwald, H.M. McConnell, *Biochemistry* 20 (1981) 4505–4510.
- [16] M.R. Vist, J.H. Davis, *Biochemistry* 29 (1989) 451–464.
- [17] J.H. Ipsen, G. Karlstrom, O.G. Mouritsen, H. Wennerstrom, M.J. Zuckermann, *Biochim. Biophys. Acta* 905 (1987) 162–172.
- [18] H.M. McConnell, *Annu. Rev. Phys. Chem.* 42 (1991) 171–195.
- [19] S.L. Keller, H.M. McConnell, *Phys. Rev. Lett.* 82 (1999) 1602–1605.
- [20] D.J. Benvegnu, H.M. McConnell, *J. Phys. Chem.* 97 (1993) 6686–6691.
- [21] A. Radhakrishnan, H.M. McConnell, *Biochemistry* 39 (2000) 8119–8124.
- [22] J.S. Rowlinson, F.L. Swinton, *Liquids and Liquid Mixtures*, 3rd ed., Butterworth Scientific, London, 1982.
- [23] J.P. Hagen, H.M. McConnell, *Biochim. Biophys. Acta* 1329 (1997) 7–11.
- [24] K.Y.C. Lee, J.F. Klingler, H.M. McConnell, *Science* 263 (1994) 655–658.
- [25] J.F. Klingler, H.M. McConnell, *J. Phys. Chem.* 97 (1993) 6096–6100.
- [26] H.A. Stone, H.M. McConnell, *Proc. R. Soc. Lond., A* 448 (1995) 97–111.
- [27] P.G. Saffman, M. Delbruck, *Proc. Natl. Acad. Sci.* 72 (1975) 3111–3113.
- [28] B. Hughes, B.A. Pailthorpe, L.R. White, *J. Fluid Mech.* 110 (1981) 349–372.
- [29] V.T. Moy, D.J. Keller, H.E. Gaub, H.M. McConnell, *J. Phys. Chem.* 90 (1986) 3198–3202.
- [30] O. Albrecht, H. Gruler, E. Sackmann, *J. Colloid Interface Sci.* 79 (1981) 319–338.
- [31] A. Radhakrishnan, H.M. McConnell, *J. Am. Chem. Soc.* 121 (1999) 486–487.
- [32] A. Radhakrishnan, H.M. McConnell, *Biophys. J.* 77 (1999) 1507–1517.
- [33] L.R. Corrales, J.C. Wheeler, *J. Chem. Phys.* 91 (1989) 7097–7112.
- [34] V. Talanquer, *J. Chem. Phys.* 96 (1992) 5408–5421.
- [35] Y. Hueda, M.E. Costas, R.L. Scott, *J. Phys. Chem., B* 101 (1997) 8676–8682.
- [36] S.L. Keller, A. Radhakrishnan, H.M. McConnell, *J. Phys. Chem., B* 104 (2000) 7522–7527.
- [37] A. Radhakrishnan, H.M. McConnell, *Proc. Natl. Acad. Sci. U. S. A.* 97 (2000) 1073–1078.
- [38] M.C. Phillips, *Prog. Surf. Membr. Sci.* 5 (1972) 139–221.
- [39] J.M. Smaby, H.L. Brockman, R.E. Brown, *Biochemistry* 33 (1994) 9135–9142.
- [40] A. Radhakrishnan, H.M. McConnell, *J. Phys. Chem.* 106 (2002) 4755–4762.
- [41] D. Marsh, *Biochim. Biophys. Acta* 1286 (1996) 183–223.
- [42] S.A. Pandit, M.L. Berkowitz, *Biophys. J.* 82 (2002) 1818–1827.
- [43] T.P.W. McMullen, R.N.A.H. Lewis, R.N. McElhaney, *Biochemistry* 32 (1993) 516–522.
- [44] T.P.W. McMullen, N.A.H. Ruthven, R.N. Lewis, R.N. McElhaney, *Biochim. Biophys. Acta* 1416 (1999) 119–134.
- [45] T.G. Anderson, H.M. McConnell, *Biophys. J.* 81 (2001) 2774–2785.
- [46] D.M. Small, *The Physical Chemistry of Lipids*, vol. 4, Plenum, New York, 1986.
- [47] J.F. Nagle, S. Tristram-Nagle, *Biochim. Biophys. Acta* 1469 (2000) 159–195.
- [48] C.A. Helm, P. Tippmann-Krayer, H. Möhwald, J. Als-Nielsen, K. Kjaer, *Biophys. J.* 60 (1991) 1475–1476.
- [49] R.P. Rand, V. Luzzati, *Biophys. J.* 8 (1968) 125–137.
- [50] A. Radhakrishnan, X.-M. Li, R.E. Brown, H.M. McConnell, *Biochim. Biophys. Acta* 1511 (2001) 1–6.
- [51] T.G. Anderson, H.M. McConnell, *Biophys. J.* 83 (2002) 2039–2052.
- [52] T.G. Anderson, H.M. McConnell, *Colloids Surf., A* 171 (2000) 13–23.
- [53] R.M. Weis, H.M. McConnell, *J. Phys. Chem.* 89 (1985) 4453–4459.

- [54] V.M. Kaganer, H. Möhwald, P. Dutta, *Rev. Mod. Phys.* 71 (1999) 779–819.
- [55] P. Somerharju, J.A. Virtanen, K.H. Cheng, *Biochim. Biophys. Acta* 1440 (1999) 32–48.
- [56] K. Tajima, N.L. Gershfeld, *Biophys. J.* 22 (1978) 489–500.
- [57] A.V. Samsonov, I. Mihalyov, F.S. Cohen, *Biophys. J.* 81 (2001) 1486–1500.
- [58] C. Dietrich, L.A. Bagatolli, Z.N. Volovyk, N.L. Thompson, M. Levi, K. Jacobson, E. Gratton, *Biophys. J.* 80 (2001) 1417–1428.
- [59] S.L. Veatch, S.L. Keller, *Phys. Rev. Lett.* 89 (2002) 268101.
- [60] R. Lipowsky, E. Sackmann, in: A.J. Hoff (Ed.), *Handbook of Biological Physics*, vol. 1B, North-Holland, Amsterdam, 1995, pp. 403–463.
- [61] H. Okamoto, *J. Phase Equilib.* 14 (1993) 336–340.
- [62] A. Radhakrishnan, H.M. McConnell, *Proc. Natl. Acad. Sci. U. S. A.* 99 (2002) 13391–13396.
- [63] D.P. Fraser, M.J. Zuckermann, O.G. Mouritsen, *Phys. Rev., A* 43 (1991) 6642–6656.
- [64] L. Miao, M. Nielsen, J. Thewalt, J.H. Ipsen, M. Bloom, M.J. Zuckerman, O.G. Mouritsen, *Biophys. J.* 82 (2002) 1429–1444.
- [65] K. Simons, E. Ikonen, *Nature* 387 (1997) 569–572.
- [66] D.A. Brown, E. London, *Annu. Rev. Cell Dev. Biol.* 14 (1998) 111–136.
- [67] D.A. Brown, E. London, *J. Membr. Biol.* 164 (1998) 103–114.
- [68] K. Simons, D. Toomre, *Nat. Rev., Mol. Cell Biol.* 1 (2000) 31–39.
- [69] H. Sprong, P. van der Sluijs, G. van Meer, *Nat. Rev., Mol. Cell Biol.* 21 (2001) 504–513.
- [70] R.G.W. Anderson, *Ann. Rev. Biochem.* 67 (1998) 199–225.
- [71] E.D. Sheets, D. Holowka, B. Baird, *Curr. Opin. Chem. Biol.* 3 (1999) 95–99.
- [72] G.J. Schütz, G. Kada, V.P. Pastushenko, H. Schindler, *EMBO J.* 19 (2000) 892–901.
- [73] A. Pralle, P. Keller, E.L. Florin, K. Simons, J.K.H. Horber, *J. Cell Biol.* 148 (2000) 997–1007.
- [74] A. Radhakrishnan, T.G. Anderson, H.M. McConnell, *Proc. Natl. Acad. Sci. U. S. A.* 97 (2000) 12422–12427.
- [75] O.H. Griffith, J.R. Brotherton, P.C. Jost, in: P.C. Jost, O.H. Griffith (Eds.), *Lipid–Protein Interactions*, vol. 2, Wiley, New York, 1982, pp. 225–237.
- [76] D. Marsh, A. Watts, in: P.C. Jost, O.H. Griffith (Eds.), *Lipid–Protein Interactions*, vol. 2, Wiley, New York, 1982, pp. 53–126.
- [77] D.W. Grainger, A. Reichert, H. Ringsdorf, C. Salesse, *FEBS Lett.* 252 (1989) 73–82.
- [78] R.C. Sarasij, M. Rao, *Phys. Rev. Lett.* 88 (2002) 088101–088101-4.
- [79] P.C. Jost, O.H. Griffith, in: P.F. Agris (Ed.), *Biomolecular Structure and Function*, Academic Press, New York, 1978, pp. 25–54.
- [80] D. Marsh, T. Pali, L.I. Horvath, in: L.J. Berliner (Ed.), *Biological Magnetic Resonance*, vol. 14, Plenum, New York, 1998, pp. 23–80.
- [81] G.B. Warren, M.D. Houslay, J.C. Metcalfe, N.J.M. Birdsall, *Nature* 255 (1975) 684–687.
- [82] R.G.W. Anderson, K. Jacobson, *Science* 296 (2002) 1821–1825.
- [83] M.S. Bretscher, S. Munro, *Science* 261 (1993) 1280–1281.
- [84] Y. Lange, T.L. Steck, *Trends Cell Biol.* 6 (1996) 205–208.
- [85] M.S. Brown, J.L. Goldstein, *Proc. Natl. Acad. Sci. U. S. A.* 96 (1999) 11041–11048.
- [86] C.B. Kallen, J.T. Billheimer, S.A. Summers, S.E. Stayrook, M. Lewis, J.F. Strauss, *J. Biol. Chem.* 273 (1998) 26285–26288.
- [87] J.P. Slotte, E.L. Bierman, *Biochem. J.* 250 (1988) 653–658.
- [88] X. Xu, I. Tabas, *J. Biol. Chem.* 266 (1991) 17040–17048.
- [89] Y. Lange, Y. Jin, M. Rigney, T.L. Steck, *J. Lipid Res.* 40 (1999) 2264–2270.
- [90] S. Scheek, M.S. Brown, J.L. Goldstein, *Proc. Natl. Acad. Sci. U. S. A.* 94 (1997) 11179–11183.
- [91] M.P. Haynes, M.C. Phillips, G.H. Rothblat, *Biochemistry* 39 (2000) 4508–4517.
- [92] L.M. Smith, J.L. Rubenstein, J.W. Parce, H.M. McConnell, *Biochemistry* 19 (1980) 5907–5911.
- [93] R. Varma, S. Mayor, *Nature* 394 (1998) 798–801.
- [94] A.K. Kenworthy, N. Petranova, M. Edidin, *Mol. Biol. Cell* 11 (2000) 1645–1655.